ChemPubSoc Europe

DOI: 10.1002/cssc.201500255

CHEMSUSCHEM Communications

Selective Oxidation of 1,6-Hexanediol to 6-Hydroxycaproic Acid over Reusable Hydrotalcite-Supported Au–Pd Bimetallic Catalysts

Jaya Tuteja, Shun Nishimura, Hemant Choudhary, and Kohki Ebitani*[a]

Selective oxidation of 1,6-hexanediol into 6-hydroxycaproic acid was achieved over hydrotalcite-supported Au–Pd bimetallic nanoparticles as heterogeneous catalyst using aqueous H_2O_2. *N*,*N*-dimethyldodecylamine *N*-oxide (DDAO) was used as an efficient capping agent. Spectroscopic analyses by UV/Vis, TEM, XPS, and X-ray absorption spectroscopy suggested that interactions between gold and palladium atoms are responsible for the high activity of the reusable $Au_{40}Pd_{60}$-DDAO/HT catalyst.

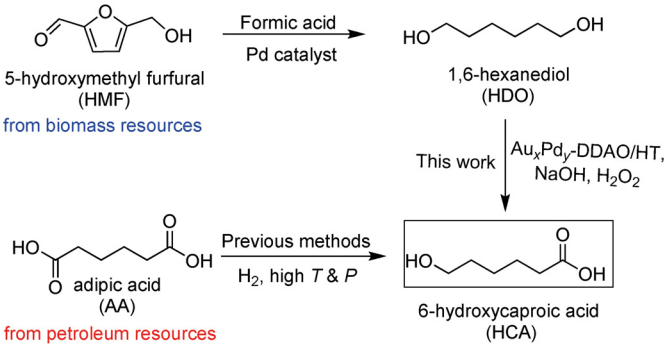

Scheme 1. Synthesis of HCA from HMF and AA.

To ensure a sustainable future for the chemical industry, a continuous supply of feedstocks from renewable sources (e.g., biomass) rather than from depleting nonrenewable petroleum sources is required.[1] Among the diverse routes of biomass utilization, selective oxidation is of significant importance for the production of valuable chemicals and intermediates, from an industrial as well as academic point of view.[2] One compound of immense value is 6-hydroxycaproic acid (HCA). HCA has potential applications in dermopharmaceuticals, cosmetics, and in the polymer industry for the production of poly(caprolactone).[3]

The classical route towards HCA includes metal-catalyzed i) reduction of adipic acid (AA) at 523 K with 300 bar H_2,[4] and ii) oxidation of cyclohexane and cyclohexanone (derivatives of fossil resources) byproducts.[5] The synthesis of HCA from renewable sources by heterogeneous catalysis is certainly desirable. This work focuses on HCA synthesis by the selective oxidation of 1,6-hexanediol (HDO), which can be directly obtained from 5-hydroxymethylfurfural (HMF, a biomass resource) by using heterogeneous catalysts (Scheme 1).[6] It has been previously reported that the selective oxidation of primary aliphatic diols gradually become difficult as the length of the carbon chain or alkyl group between the two hydroxyl groups increases when using Pt/C catalyst with acetic acid as additive at 343 K under 10 bar O_2.[7] Other researchers have also discussed complications involved in the selective oxidation of long-chain aliphatic diols.[8]

During the last 2–3 decades, many efforts to produce active and selective heterogeneous catalysts have been made. Among these, metal nanoparticle (NP)-based heterogeneous catalysts have been extensively investigated.[9] In general, the nature of the capping agent affects the chemical and physical properties of metal NPs.[10] Recently, bimetallic NPs with capping agents have gained significant attention owing to their novel catalytic properties, which are different from their monometallic counterparts.[11] Among them, the catalysis of bimetallic Au–Pd has been widely explored for oxidations of alcohols,[11] methane,[12] and CO.[13] Kishida et al. (in 2010[14]) and our research group (very recently[15]) utilized *N*,*N*-dimethyldodecylamine *N*-oxide (DDAO; Supporting Information, Figure S1) as a capping agent for the synthesis of silver nanowires and Co–Pd NPs, respectively.

Herein, we extend the scope of DDAO for the preparation of Au–Pd bimetallic NPs supported on hydrotalcite (HT)[16] for selective oxidation of HDO to HCA under mild conditions, which has not been reported previously.

A series of Au–Pd bimetallic NPs was prepared with DDAO by using a modified polyol reduction method (see Supporting Information).[10c] The resultant NPs were supported on HT (Mg/Al = 5.4) and denoted as Au_xPd_y-DDAO/HT, where *x* and *y* represents the molar ratio of gold and palladium, respectively. Both monometallic and bimetallic HT-supported NP catalysts were tested for the oxidation of HDO to HCA at 353 K under alkaline medium with 30% aq H_2O_2 as oxidant.[17] Table 1 summarizes the results for HDO oxidation together with the average particle size and actual metal loading as measured by transmission electron microscopy (TEM) and inductively coupled plasma–atomic emission spectrometry (ICP–AES), respectively. The average particle size was around 4–6 nm, except for monometallic Au_{100}-DDAO/HT (28.4 nm; Supporting Information, Figure S2a), which showed an extremely low activity

[a] *J. Tuteja, Dr. S. Nishimura, H. Choudhary, Prof. Dr. K. Ebitani*
School of Materials Science
Japan Advanced Institute of Science and Technology
1-1 Asahidai, Nomi, Ishikawa 923-1292 (Japan)
Fax: (+81) 761-51-1149
E-mail: ebitani@jaist.ac.jp

Supporting Information for this article is available on the WWW under http://dx.doi.org/10.1002/cssc.201500255.

Table 1. Screening the Au/Pd metal ratio of DDAO-stabilized Au_xPd_y in the oxidation of HDO into HCA.[a]

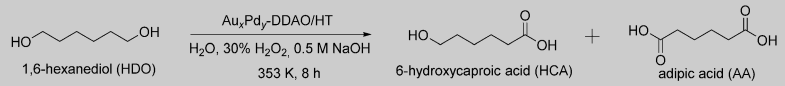

Entry	Catalyst	HDO conversion[b] [%]	Yield (sel.)[b] [%] HCA	AA	Actual metal loading $\times 10^{-3}$ [mmol g^{-1}][c] Au	Pd	TON[d]	Average size [nm][e]
1	Au_{100}-DDAO/HT	18	12 (67)	0 (0)	93.2		27	28.4
2	$Au_{80}Pd_{20}$-DDAO/HT	86	45 (52)	10 (12)	72.2	16.2	100	6.2
3	$Au_{60}Pd_{40}$-DDAO/HT	90	72 (80)	6 (7)	50.6	34.0	170	4.7
4	$Au_{40}Pd_{60}$-DDAO/HT	87, 87[f]	81, 80[f] (93, 92[f])	4, 4[f] (5, 5[f])	33.7	55.6	184	4.2
5	$Au_{20}Pd_{80}$-DDAO/HT	36	8 (22)	0 (0)	17.4	71.7	19	4.5
6	Pd_{100}-DDAO/HT	10	7 (70)	0 (0)		89.4	16	4.8
7	$Au_{40}Pd_{60}$-DDAO/HT[g]	38	24 (63)	1 (3)				–
8	$Au_{40}Pd_{60}$-DDAO/HT[h]	12	9 (75)	0 (0)				–
9	blank	7	5 (71)	0 (0)				–

[a] Reaction conditions: HDO (0.5 mmol), catalyst (25 mg, Au + Pd = 0.0025 mmol), 30% aq. H_2O_2 (0.75 mL, 6 mmol), 0.5 M NaOH (0.75 mL), H_2O (3.5 mL), 353 K, 8 h. [b] Analyzed by HPLC (see Supporting Information). [c] Estimated with ICP-AES analysis. [d] Calculated based on total metal amount. [e] Determined by TEM. [f] With QuadraPure TU (33.4 mg). [g] Without 30% aq. H_2O_2. [h] Without 0.5 M NaOH.

(entry 1). Also, a monometallic palladium catalyst (Pd_{100}-DDAO/HT) with a particle size of 4.8 nm had a low HCA yield (entry 6). Interestingly, the co-presence of gold and palladium (Au_xPd_y-DDAO/HT) bimetallic catalysts dramatically enhanced the HCA yield and selectivity (entries 2–5). Among the various Au_xPd_y-DDAO/HT catalysts, $Au_{40}Pd_{60}$-DDAO/HT possessed the highest catalytic activity, with 81% HCA yield (93% selectivity). AA was the only byproduct observed using these catalysts.[18] A remarkable difference in the catalytic behavior for oxidation of HDO to HCA was observed with the change in Au/Pd molar ratio (Table 1), which did not have a significant effect on the particle size distribution of the Au_xPd_y-DDAO/HT catalysts. These results indicate the important role of synergistic interactions between gold and palladium for the excellent catalytic performance of the $Au_{40}Pd_{60}$-DDAO/HT materials.

The presence of NaOH and H_2O_2 is crucial to effect the above-mentioned high catalytic activity, as the absence of any of them leads to low HCA yields (Table 1; entries 7–9). The catalytic activity of the $Au_{40}Pd_{60}$-DDAO/HT was noticed to be strongly influenced by the amounts of base and oxidant added (Supporting Information, Table S1), 6 mmol of 30% aq. H_2O_2 and 0.75 mL of 0.5 M NaOH was found to afford the highest HCA yield of 81% with 87% HDO conversion (Table S1, entry 13). The catalytic activity of $Au_{40}Pd_{60}$-DDAO/HT was compared with analogous Au–Pd nanoparticles on other supports to identify their role (Supporting Information, Table S3). Although all catalysts promoted the formation of HCA to some extent, $Au_{40}Pd_{60}$-DDAO/HT stood out with the highest catalytic activity, perhaps the basic sites of HT help in enhancing the catalytic performance as compared to neutral and/or less-strongly-basic supports.

The product was isolated (Supporting Information) as an oily liquid (81.7% isolated yield), and ^{1}H-, ^{13}C NMR confirmed the structure of HCA (Figure S3). In addition, the same catalyst could also promote the oxidation of HDO at 5 mmol scale with similar efficiency to reach a high TON of 265 (Supporting Information, Table S2).

An important issue for heterogeneous catalytic systems is the possibility of metal leaching into the reaction mixture, and catalyst reusability. We found the catalyst to be highly reusable, up to at least 5 times without any further treatment (Figure 1). The reaction did not proceed when the catalyst was filtered off after 2 h (Supporting Information, Figure S4). Moreover, ICP–AES analysis of the filtrate demonstrated that neither gold nor palladium had leached into the solution. In addition, the presence of QuadraPure TU, known as a scavenger of homogeneous metal species,[19] did not influence the catalytic activity (Table 1; entry 4f). These experiments authenticate the heterogeneous nature of the $Au_{40}Pd_{60}$-DDAO/HT catalyst under our reaction conditions.

A comparison of X-ray diffraction (XRD) patterns and TEM images of the fresh and spent $Au_{40}Pd_{60}$-DDAO/HT catalysts

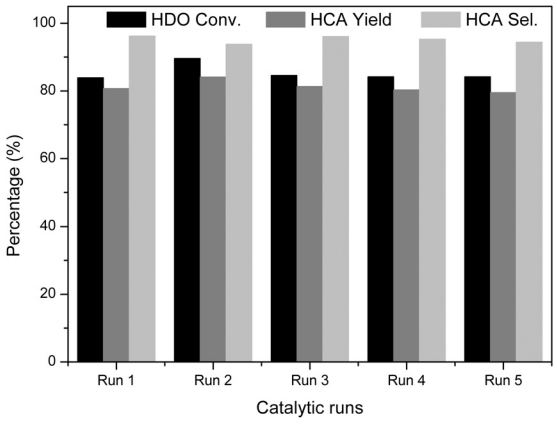

Figure 1. Recyclability of catalyst for selective oxidation of HDO to HCA. Reaction Conditions: HDO (0.5 mmol), $Au_{40}Pd_{60}$-DDAO/HT (25 mg), 0.5 M NaOH (0.75 mmol), 30% H_2O_2 (0.75 mL), H_2O (3.5 mL), 353 K, 8 h, 500 rpm.

(Supporting Information, Figures S5 and S2, respectively) revealed that there is no significant change in the catalyst morphology. The AuPd NPs were homogeneously dispersed on the HT surface even after the reaction, with a slight increase of the mean size of the NPs from 4.2 to 4.8 nm. Au L_{III}-edge and Pd K-edge XANES and EXAFS results also suggested robust local structure around gold and palladium after the reaction (Supporting Information, Figure S6), indicating that the DDAO-capped bimetallic AuPd NPs are stable under these reaction conditions.

To study the reaction pathway, the reaction over the $Au_{40}Pd_{60}$-DDAO/HT catalyst was performed in the presence of melatonin, a water-soluble radical scavenger of hydroxyl radicals ($OH^{\cdot}$).[20] The presence of melatonin (0.3 mmol) prohibited the selective oxidation of HDO (5% yield of HCA, with traces of AA), suggesting a radical pathway under the present reaction conditions. The formation of radicals over metal NPs in the presence of hydrogen peroxide has been reported previously,[21] and this seems to play a key role during the HDO oxidation.

To understand the superiority of the $Au_{40}Pd_{60}$-DDAO/HT catalyst, the series of Au–Pd bimetallic catalysts was characterized by means of various spectroscopic methods. Figure S7 (Supporting Information) shows representative UV/Vis spectra of monometallic and Au–Pd bimetallic catalysts. The monometallic gold catalyst exhibited a characteristic surface plasmon resonance (SPR) absorption peak at 524 nm, due to Au NPs.[22] Admixing of palladium to gold strongly diminished the SPR absorption peak, and a very weak peak can be observed in the spectra of $Au_{80}Pd_{20}$-DDAO/HT and $Au_{60}Pd_{40}$-DDAO/HT. Over the entire spectral range, no SPR absorption peak is distinct in the spectra of $Au_{40}Pd_{60}$-DDAO/HT, $Au_{20}Pd_{80}$-DDAO/HT, and Pd_{100}-DDAO/HT. The weakening SPR band in the bimetallic samples can be attributed to interactions between gold and palladium species, rather than to the formation of separate gold and palladium NPs and a gold "mother" surface.[10c]

The interaction between palladium and gold atoms was studied by X-ray photoelectron spectroscopy (XPS). Figure 2 shows XPS results of core-level binding energies (BEs) for Au4f

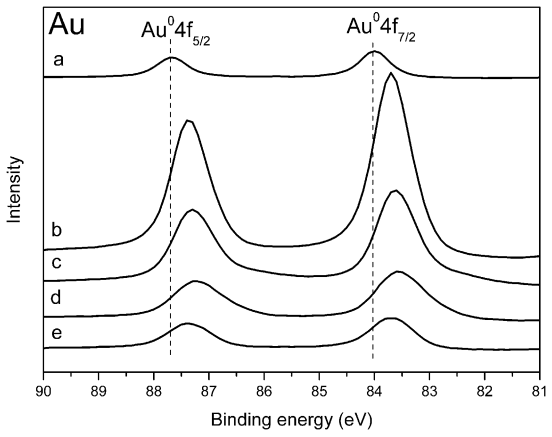

Figure 2. Au 4f XPS spectra of Au_xPd_y-DDAO NPs. (a) Au_{100}-DDAO NPs, (b) $Au_{80}Pd_{20}$-DDAO NPs, (c) $Au_{60}Pd_{40}$-DDAO NPs, (d) $Au_{40}Pd_{60}$-DDAO NPs, (e) $Au_{20}Pd_{80}$-DDAO NPs.

of the Au_xPd_y-DDAO NPs. The BEs of Au $4f_{5/2}$ (87.7 eV) and Au $4f_{7/2}$ (84.0 eV) in the Au_{100}-DDAO NPs are assigned to Au 4f orbitals in metallic gold.[13,24] A clear negative shift in BE for Au 4f was observed for Au–Pd samples. The maximum shift of −0.5 eV relative to the BE of pure gold NPs was observed for the $Au_{40}Pd_{60}$-DDAO NPs. This negative BE shift is an indication of an increase in the electron density on gold to form negatively-charged gold species, suggesting a modification of the electronic structure in the presence of palladium. In the case of Pd 3d XPS, the BE of Au–Pd bimetallic NPs also shifted towards lower energy (Supporting Information, Figure S8); that is, exhibiting a negative BE shift with increase in gold content due to the gaining of d-electrons, from gold. These shifts towards lower BEs for both Pd $3d_{3/2}$ and Au $4f_{7/2}$ are consistent with a net charge flowing into gold and palladium upon Au–Pd alloying. The same phenomenon has been observed by various researchers.[13,24] A large shift for Au $4f_{7/2}$ (−0.5 eV) and for Pd $3d_{3/2}$ (−0.3 eV) in the $Au_{40}Pd_{60}$-DDAO NPs suggests the strongest interaction between gold and palladium at this molar ratio.

Further investigations on the nature of supported Au–Pd bimetallic nanoparticles were conducted by X-ray adsorption spectroscopy (XAS) of the Au L_{III}-edge, and Pd K- and L_{III}-edges. The Au L_{III}-edge XANES spectra of Au_xPd_y-DDAO/HT catalysts together with gold foil are shown in Figure 3. The white line

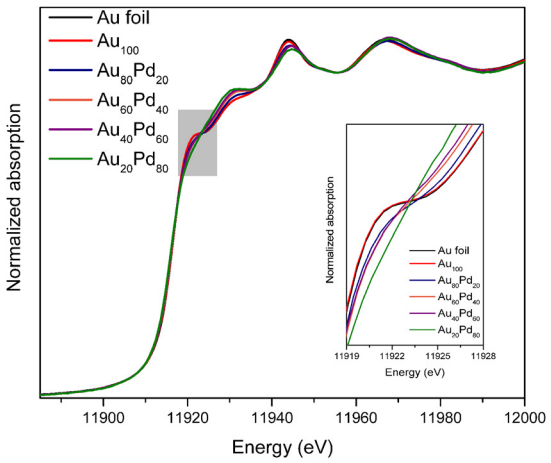

Figure 3. Au L_{III}-edge XANES of Au_xPd_y-DDAO/HT. The inset magnifies the white-line region.

(WL) intensity, the first feature after edge jump, decreases for Au–Pd bimetallic catalysts with increase in palladium content, and almost disappears for $Au_{20}Pd_{80}$-DDAO/HT. This decrease in the intensity implies that the d-electron density of gold has been increased in Au–Pd bimetallic NPs, as compared to gold foil or the Au_{100}-DDAO/HT.[10(c),25] The increase in the d-electron density of gold is due to Au–Pd d–d interactions or Au–Pd bond formation.[26,27] In addition, the intensity of second band just after the WL feature (11 935 eV) is more prominent with higher palladium content, which suggests interactions between gold and palladium atoms.[24(b),26]

A Fourier transform (FT) of the Au L_{III}-edge EXAFS spectra is plotted in Figure S9(B) (Supporting Information). The Au–Pd bimetallic catalysts showed intense doublet peaks at 2.1 and 2.9 Å as compared to gold foil and Au_{100}-DDAO/HT. The appearance and intensification of the doublet with increase in palladium content is an indication of Au–Pd bonds[24a,25b] in Au–Pd bimetallic NP-based heterogeneous catalysts.[28] The palladium XAS features in K- and L_{III}-edges (Supporting Information, Figure S10) also supports the notion of strong correlations between palladium and gold. The two features at 24389 and 24428 eV in the Pd K-edge XANES spectra are found at lower energy for Au–Pd bimetallic catalysts than for palladium foil [Figure S10(A)].[29] Furthermore, the FT of Pd K-edge EXAFS spectra [Supporting Information, Figure S11(B)] shows splitting of the peak at 2–3 Å with increase in gold content.[30] These shifts can be attributed to changes in electronic structure around palladium by alloying with gold.[26] From these observations, we infer that the electronic properties of gold and palladium are significantly changed in the bimetallic catalysts as a consequence of Au–Pd interactions (bond formation). These particular interactions or Au–Pd nanoalloy centers may be responsible for the high catalytic activity of $Au_{40}Pd_{60}$-DDAO/HT in the selective oxidation of HDO to HCA.

In summary, a series of hydrotalcite-supported *N*,*N*-dimethyldodecylamine *N*-oxide (DDAO)-capped bimetallic Au–Pd nanoparticles are prepared, and their catalytic activities are explored for oxidation of 1,6-hexanediol (HDO) to 6-hydroxycaproic acid (HCA). A maximum HCA yield of 81% at an HDO conversion of 87% was achieved with a reusable $Au_{40}Pd_{60}$-DDAO/HT catalyst in basic aqueous media using H_2O_2. Spectroscopic investigations suggest that interactions between gold and palladium provide the active sites responsible for selective oxidation of the primary OH group of the C6 aliphatic diol, HDO.

Acknowledgements

This work was partially supported by a Young Scientists (B) grant (25820392) and a Grant-in-Aid for Scientific Research (C) (25420825) of the Ministry of Education, Culture, Sports, Science and Technology (MEXT), Japan. H.C. thanks JSPS for a fellowship. XAS was performed at the BL-9C (Au L_{III}-edge) and the BL-9A (Pd L_{III}-edge) of Photon Factory at High Energy Accelerator Research Organization (KEK-PF), Tsukuba, Japan, under Proposals 2013G586 and 2012G763. The BL01B1 in the SPring-8 with the approval of the Japan Synchrotron Radiation Research Institute (JASRI) (2014B1472) was also used for Pd K-edge XAS studies.

Keywords: gold · hydrotalcites · oxidation · palladium · renewable resources

[1] For Example: a) G. W. Huber, J. N. Chheda, C. J. Barrett, J. A. Dumesic, *Science* **2005**, *308*, 1446–1450; b) J. C. Serrano-Ruiz, R. Luque, A. Sepúlveda-Escribano, *Chem. Soc. Rev.* **2011**, *40*, 5266–5281; c) P. Gallezot, *Chem. Soc. Rev.* **2012**, *41*, 1538–1558.

[2] a) F. Jin, H. Enomoto, *Energy Environ. Sci.* **2011**, *4*, 382–397; b) N. K. Gupta, S. Nishimura, A. Takagaki, K. Ebitani, *Green Chem.* **2011**, *13*, 824–827; c) M. Besson, P. Gallezot, C. Pinel, *Chem. Rev.* **2014**, *114*, 1827–1870; d) H. Choudhary, S. Nishimura, K. Ebitani, *Appl. Catal. B* **2015**, *162*, 1–10.

[3] a) M. Labet, W. Thielemans, *Chem. Soc. Rev.* **2009**, *38*, 3484–3504; b) R. Orchel, K. Jelonek, J. Kasperczyk, Z. Dzierøewicz, *Acta Pol. Pharm.-Drug Res.* **2010**, *67*, 710–714; c) A. Georgia, *Lactates-Advances in Research and Application* (Eds.: Q. A. Acton), Scholarly Edition, **2013**, pp. 127.

[4] R. H. Fischer, R. Pinkos, F. Stein, US6426438 B1, **2002**.

[5] a) I. Belkhir, A. Germain, F. Fajula, E. Fache, *Studies in Surface Science and Catalysis* (Eds.: S. T. Oyama, A. M. Gaffney, J. E. Lyons, R. K. Grasselli), Third World Congress on Oxidation Catalysis, Elsevier, **1997**, pp. 577; b) N. d'Alessandro, L. Liberatore, L. Tonucci, A. Morvillo, M. Bressan, *New J. Chem.* **2001**, *25*, 1319–1324; c) Y. Usui, K. Sato, *Green Chem.* **2003**, *5*, 373–375.

[6] a) T. Buntara, S. Noel, P. H. Phua, I. M. Cabrera, J. G. de Vries, H. J. Heeres, *Angew. Chem. Int. Ed.* **2011**, *50*, 7083–7087; *Angew. Chem.* **2011**, *123*, 7221–7225; b) M. Chia, Y. J. P-Torres, D. Hibbittts, Q. Tan, H. N. Pham, A. K. Datye, M. Neurock, R. J. Davis, J. A. Dumesic, *J. Am. Chem. Soc.* **2011**, *133*, 12675–12689; c) J. Tuteja, H. Choudhary, S. Nishimura, K. Ebitani, *ChemSusChem* **2014**, *7*, 96–100.

[7] M. S. Ide, R. J. Davis, *J. Catal.* **2013**, *308*, 50–59.

[8] a) H. Tohma, T. Maegawa, S. Takizawa, Y. Kita, *Adv. Synth. Catal.* **2002**, *344*, 328–337; b) S. Kara, D. Spickermann, J. H. Schrittwieser, A. Weckbecker, C. Leggewie, I. W. C. E. Arends, F. Hollmann, *ACS Catal.* **2013**, *3*, 2436–2439.

[9] a) S. Schauermann, N. Nilius, S. Shaikhutdinov, H.-J. Freund, *Acc. Chem. Res.* **2013**, *46*, 1673–1681; b) Z. Guo, B. Liu, Q. Zhang, W. Deng, Y. Wang, Y. Yang, *Chem. Soc. Rev.* **2014**, *43*, 3480–3524.

[10] a) D. I. Enache, J. K. Edwards, P. Landon, B. Solsona-Espiru, A. F. Carley, A. A. Herzing, M. Watanabe, C. J. Kiely, D. W. Knight, G. J. Hutchings, *Science* **2006**, *311*, 362–365; b) H. Zhang, T. Watanabe, M. Okumura, M. Haruta, N. Toshima, *Nat. Mater.* **2012**, *11*, 49–52; c) S. Nishimura, Y. Yakita, M. Katayama, K. Higashimine, K. Ebitani, *Catal. Sci. Technol.* **2013**, *3*, 351–359; d) D. Tongsakul, S. Nishimura, K. Ebitani, *J. Phys. Chem. C* **2014**, *118*, 11723–11730.

[11] a) N. Toshima, T. Yonezawa, *New J. Chem.* **1998**, *22*, 1179–1201; b) H. B. Liu, U. Pal, A. Medina, C. Maldonado, J. A. Ascencio, *Phys. Rev. B* **2005**, *71*, 075403-1–075403-6; c) A. Villa, M. Schiavoni, S. Campisi, G. M. Veith, L. Prati, *ChemSusChem* **2013**, *6*, 609–612.

[12] M. H. Ab Rahim, M. M. Forde, R. L. Jenkins, C. Hammond, N. Dimitratos, J. A. Lopez-Sanchez, A. F. Carley, S. H. Taylor, D. J. Willock, D. Murphy, C. J. Kiely, G. J. Hutchings, *Angew. Chem. Int. Ed.* **2013**, *52*, 1280–1284; *Angew. Chem.* **2013**, *125*, 1318–1322.

[13] J. Xu, T. White, P. Li, C. H. He, J. G. Yu, W. K. Yuan, Y.-F. Han, *J. Am. Chem. Soc.* **2010**, *132*, 10398–10406.

[14] H. Matsune, Y. Kuramitsu, S. Takenaka, M. Kishida, *Chem. Lett.* **2010**, *39*, 717–719.

[15] H. Choudhary, S. Nishimura, K. Ebitani, *ChemCatChem* **2015**, 10.1002/cctc.201500161.

[16] a) B. F. Sels, D. E. De Vos, M. Buntinx, F. Pierard, A. KirschDe Measmarker, P. A. Jacobs, *Nature* **1999**, *400*, 855–857; b) K. Kaneda, K. Mori, T. Mizugaki, K. Ebitani, *Bull. Chem. Soc. Jpn.* **2006**, *79*, 981–1016; c) S. Nishimura, A. Takagaki, K. Ebitani, *Green Chem.* **2013**, *15*, 2026–2042.

[17] a) *Catalytic Oxidations with Hydrogen Peroxide as Oxidant* (Eds.: G. Strukul), Kluwer Academic, Dordrecht, The Netherlands, **1992**; b) R. Noyori, M. Aoki, K. Sato, *Chem. Commun.* **2003**, 1977–1986.

[18] The HPLC analysis of the reaction mixture denied the presence of any other water-soluble products after the reaction. Also, both ^{1}H- and ^{13}C NMR spectroscopy (Figure S3) of the reaction mixture extracted by the organic solvent (chloroform)only identified the three compounds of HDO, HCA and AA.

[19] a) J. M. Richardson, C. W. Jones, *Adv. Synth. Catal.* **2006**, *348*, 1207–1216; b) H. Choudhary, S. Nishimura, K. Ebitani, *J. Mater. Chem. A* **2014**, *2*, 18687–18696.

[20] a) H. J. Bromme, W. Morke, E. Peschke, H. Ebelt, D. Peschke, *J. Pineal Res.* **2000**, *29*, 201–208; b) M. Yoshida, A. Fukuda, M. Hara, A. Terada, Y. Kitanaka, S. Owada, *Life Sci.* **2003**, *72*, 1773–1780.

[21] a) D. W. McKee, *J. Catal.* **1969**, *14*, 355–364; b) S. Navalon, R. Martin, M. Alvaro, H. Garcia, *Angew. Chem. Int. Ed.* **2010**, *49*, 8403–8407; *Angew. Chem.* **2010**, *122*, 8581–8585.

[22] a) S. Link, M. A. El-Sayed, *J. Phys. Chem. B* **1999**, *103*, 4212–4217; b) H. Yang, D. Tang, X. Lu, Y. Yuan, *J. Phys. Chem. C* **2009**, *113*, 8186–8193.

[23] R. E. Watson, J. Hudis, M. L. Periman, *Phys. Rev. B* **1971**, *4*, 4139 – 4144.
[24] a) A. Murugadoss, K. Okumura, H. Sakurai, *J. Phys. Chem. C* **2012**, *116*, 26776 – 26783; b) R. Wang, Z. Wu, C. Chen, Z. Qin, H. Zhu, G. Wang, H. Wang, C. Wu, W. Dong, W. Fan, J. Wang, *Chem. Commun.* **2013**, *49*, 8250 – 8252; c) P. A. P. Nascente, S. G. C. Decastro, R. Landers, G. G. Kleiman, *Phys. Rev. B* **1991**, *43*, 4659 – 4666; d) M. Cini, M. Decrescenzi, F. Patella, N. Motta, M. Sastry, F. Rochet, R. Pasquali, A. Balzarotti, C. Verdozzi, *Phys. Rev. B* **1990**, *41*, 5685 – 5695.
[25] a) P. Dash, T. Bond, C. Fowler, W. Hou, N. Coombs, R. W. J. Scott, *J. Phys. Chem. C* **2009**, *113*, 12719 – 12730; b) S. Nishimura, N. Ikeda, K. Ebitani, *Catal. Today* **2014**, *232*, 89 – 98.
[26] S. Marx, A. Baiker, *J. Phys. Chem. C* **2009**, *113*, 6191 – 6201.
[27] T. Balcha, J. R. Strobl, C. Fowler, P. Dash, R. W. J. Scott, *ACS Catal.* **2011**, *1*, 425 – 436.
[28] Figure S9 (A) shows k^3-weighted Au L_{III}-edge EXAFS oscillation pattern for Au foil and catalysts. The EXAFS oscillation patters also supports the presence of AuPd heterometallic bond formation with diminishing of doublet characteristics at 5.2 $Å^{-1}$.
[29] The Pd K-edge XANES of the $Au_{40}Pd_{60}$-DDAO/HT was very close to that of Pd foil, while the height of $Au_{40}Pd_{60}$-DDAO/HT in Pd L_{III}-edge was little higher than Pd metal (Figure S10 (B)). These suggested the depletion of electron in Pd 4d state in $Au_{40}Pd_{60}$-DDAO/HT was caused by the presence of Pd-Au bonds.
[30] All the AuPd bimetallic catalysts showed similar k^3-weighted Pd K-edge EXAFS patterns to the Pd foil (Figure S11 (A)).

Received: February 17, 2015
Revised: March 25, 2015
Published online on May 20, 2015